Comparative Investigation of Spherical NF Measurements with Full and First Order Probe Correction Using Calibrated or Simulated Probe

F. Saccardi[1], A. Giacomini[1], L. J. Foged [1]
[1] Microwave Vision Italy s.r.l., Via dei Castelli Romani 59, 00071, Pomezia, Italy
francesco.saccardi@microwavevision.com, andrea.giacomini@microwavevision.com, lars.foged@microwavevision.com

***Abstract*—Accurate spherical Near-Field antenna measurements are typically performed compensating for the probe pattern during the Near-Field to Far-Field transformation. Depending on the complexity of the probe modal content and on the required accuracy, different Probe Correction (PC) techniques can be applied. It is common practice to distinguish between first order PC, where only |μ|=1 spherical modes of the probe are compensated for, and full PC, taking into account the entire probe spectrum.**

Another key factor to be considered when applying the PC is the probe characterization. In order to obtain very accurate results, it is common practice to calibrate the probe in dedicated measurement campaigns which, unfortunately, can often be time consuming and expensive. Alternatively, the simulated probe performance can be used to perform the PC. A comparative investigation between full and first order PC performed using calibrated or simulated probe is presented in this paper.

***Index Terms*— Spherical Wave Expansion, Spherical Near Field, Higher order probe, Probe Correction, Probe Calibration.**

I. Introduction

In spherical Near-Field (NF) measurements, the influence of the probe on the accuracy of the measurement results depends on the complexity of the probe pattern and on the size/displacement of the Antenna/Device Under Test (AUT/DUT) which, together with the measurement radius, can generate larger view angles. In order to obtain accurate results, in many measurement situations it is common practice to compensate for the probe effect applying a Probe Correction (PC) procedure during the Spherical Wave Expansion (SWE) of the field [1-3].

A widely used probe compensation procedure is the so-called first order PC [3] where a |μ|=1 probe is assumed. This procedure has been demonstrated to be very accurate and computationally efficient. However, it imposes stringent requirements on the probe azimuthal symmetry since only one spherical mode (|μ|=1) is to be radiated. The design of such probes is often a trade-off between achievable performance, modal purity and bandwidth [4-5]. In order to have less restriction in the selection of the probe, different full or higher order PC techniques have been recently proposed [6-12]. The full PC developed by Microwave Vision Group (MVG) is based on the modification of the SWE basis functions. Such functions are properly elaborated taking into account the effect of the (known) probe and then used in the SWE directly compensating for the probe pattern without any restriction on the probe itself. The effectiveness of such technique has been experimentally demonstrated in [11-12].

An interesting point to be addressed is the impact of the probe characterization on the overall measurement accuracy.

The signal radiated by the DUT and measured by the probe, from a mathematical point of view, can be seen as the result of the convolution between the AUT and probe spherical wave spectrum. In order to obtain the compensated AUT spectrum, a deconvolution operation is performed while applying either the first order or full PC. Of course, such deconvolution can be performed only if the probe spectrum is known. It is thus interesting to understand how accurate the probe characterization should be.

The common practice in order to obtain the probe characterization is to calibrate it in a dedicated measurement campaigns which, unfortunately may be time consuming and expensive. An alternative is to use the simulated performance of the probe which are in many cases already available because part of the design process of the probe.

In this paper, a comparative investigation between PC performed using calibrated and simulated probe is presented, taking into account a standard gain antenna as AUT and the higher order probe already considered in [12]. The investigation has been carried out considering both full and first order probe correction algorithms.

II. First Order and Full Probe Correction Techniques

First order and full PC techniques considered in this work are both applied during the spherical NF/FF transformation process involving the SWE of the measured field. In particular, in both cases, the SWE is performed taking into account the so-called transmission formula reported in (1):

$$w(r,\chi,\theta,\varphi) = \\ = 0.5 \sum_{\substack{smn \\ \sigma\mu\nu}} Q_{smn}^{(3)} e^{jm\varphi} d_{\mu m}^{n}(\theta) e^{j\mu\chi} C_{\sigma\mu\nu}^{sn(3)}(kr)\, R_{\sigma\mu\nu}^{p} \qquad (1)$$

Such formula expresses the complex signal received by a probe (w) of known coefficients ($R^{p}_{\sigma\mu\nu}$) as a function of the probes coordinates (r, θ, φ) and orientation (χ) when an AUT described by its own spherical wave coefficient ($Q^{(3)}_{smn}$) is transmitting. The symbols $d^{n}_{\mu m}(\theta)$ and $C^{sn(3)}_{\sigma\mu\nu}(kA)$ are respectively rotation and translation operators that, together with the two complex exponentials ($e^{jm\varphi}$and $e^{j\mu\chi}$), are used to describe the probe position/orientation in each measurement point.

When the first order PC is applied, only the |μ|=1 modes of the probe are taken into account. In [3] it has been demonstrated that with such assumption equation (1) can be solved in a very elegant and efficient way involving a double FFT (along both scanning axes). Unfortunately, if the probe radiates higher order modes, a residual error may affect the measured AUT pattern. This unwanted effect is known as probe modal truncation.

The full PC approach involved in this work has previously been presented in [11-12]. In order to take into account the entire spherical modal spectrum of the probe, each spherical wave function is modified through the transmission formula (1), so that the probe spectral information are already included in the expansion basis. A linear system is then set-up and inverted using the modified spherical wave functions. In [11-12] it has been also pointed out that the solution of that linear system can be made efficient involving an FFT along the φ-axis. It is remarked that this analytical approach based on the modified spherical wave basis functions leads to an effective full probe correction scheme comparable with the formulation described in [9].

III. Measurement With Higher Order Probe

The comparative investigation between PC performed with calibrated and simulated probe has been carried out taking into account a test case already considered in [12].

The measurement setup is illustrated in Fig .1. As can be seen, the MVG QH800 open boundary quad-ridge horn (see Fig. 2 and [13]) has been used as (higher order) probe. Such antenna is a reference device typically used for calibration purposes in the frequency range 0.8-12 GHz.

Besides its wide-band applicability, the interest of this antenna regarding its usage as measurement probes is due to its robustness, stability and repeatability. Furthermore, it is also a dual polarized device, making it even more appealing, since two orthogonal field components can be measured simultaneously.

The AUT is the MVG SGH820, a standard gain horn working at X-Band. The aperture dimensions of the SGH820 are 198x148 mm, while the AUT height is 353 mm. Such antenna is electrically large enough to enhance the distortion of the radiated field measured by the probe.

Measurements have been performed in the Italian office of MVG sited in Pomezia (Rome), using a robotic arm system [14] already involved in other activities [15]. Such a robot can be programmed to perform different scanning schemes (e.g. planar, spherical). For this measurement validation campaign, hemispherical NF measurements have been performed placing the AUT on the robotic arm and the probe on a tower located in front of the robot as illustrated in Fig. 1.

The alignment of the AUT and probe positioners is provided by sliding the probe tower in proximity of the robot and mating the AUT and probe interfaces with a precision mechanical adaptor.

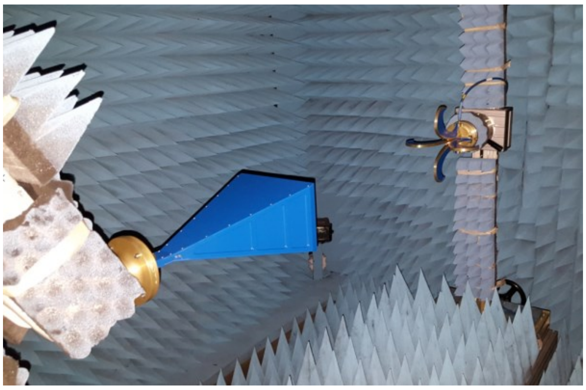

Fig. 1. MVG SGH820 during measurement with MVG QH800 higher order probe.

A reference measurement has been performed using the MVG DOEW6000 as probe [16]. As shown in [11], the DOEW6000 is a first order probe (it only radiates |μ|=1 azimuthal modes) and has a directivity of approximately 10 dBi @ 12GHz. Measurements have been conducted with the interface of the AUT corresponding to the center of rotation. Based on this displacement and on the AUT dimension, a sampling step of 1.5° along the θ-axis and of 5° along the φ-axis have been chosen. The measurement radius (distance from the center of rotation and the probe aperture) is approximately 1.1m.

Reference FF data have been obtained applying the NF/FF transformation including first order probe correction to the NF data acquired with the above described setup.

Using the same measurement setup, hemispherical NF measurements of the same AUT have been performed also using the QH800 higher order probe mentioned above (see Fig. 2). Despite the dual-polarization of the antenna, for the sake of simplicity of the measurement setup, data have been collected involving only one port.

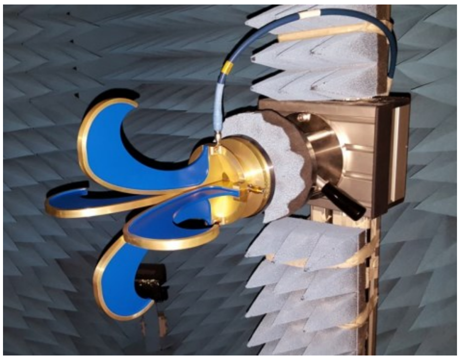

Fig. 2. MVG QH800 open boundary quad-ridge hord used as (higher order) probe.

A. Probe Characterization

The QH800 higher order probe has been calibrated in the same hemispherical measurement setup described above. The QH800 has been mounted on the robotic arm and it has been measured with the DOEW6000 first order probe. Radiation patterns and spherical wave spectrum of the QH800 have been obtained applying the NF/FF transformation (including first order PC) to the measured data.

Using full-wave simulations [17] another probe representation in terms of radiation pattern and spherical wave spectrum have also been obtained.

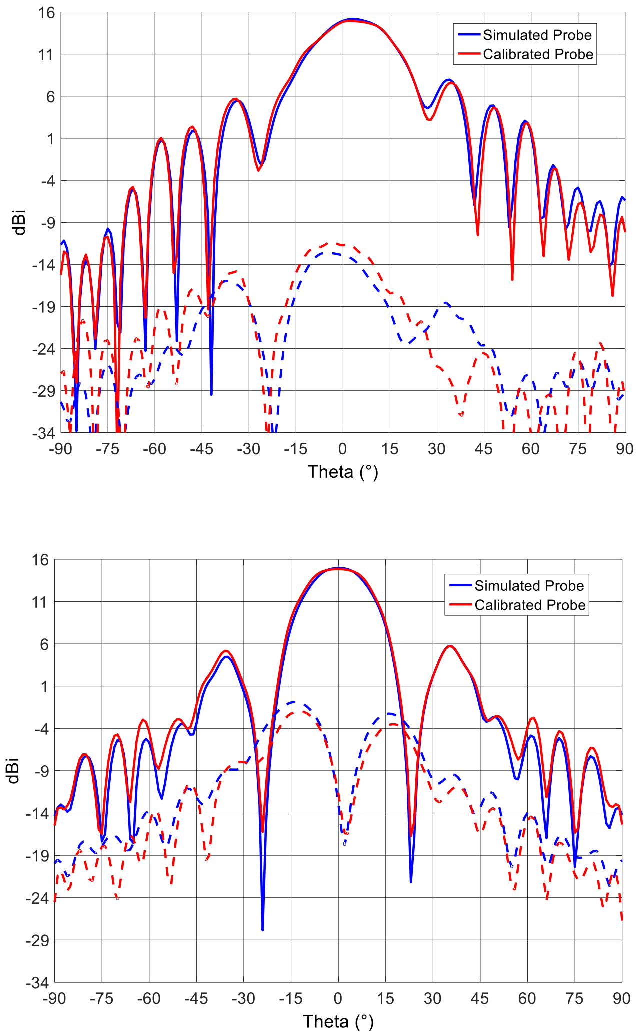

Fig. 3. Measured vs. calibrated directivity pattern of the MVG QH800 higher order probe: E-plane (top), H-Plane (bottom).

The comparison between calibrated and simulated probe directivity patterns @ 12GHz is reported in Fig. 3 (solid and dashed lines represent the co-polar and cx-polar components respectively). Similarly, the spherical wave spectrum comparison between data coming from measurement and simulation are shown on Fig. 4.

The agreement between the two different representations of the probe is excellent in terms of both co/cx-polar pattern and spherical modal content. The QH800, being a reference antenna fully manufactured by precision machining from solid aluminum, is in fact a very stable and repeatable device. Its performances can be predicted with high confidence through proper full-wave simulations.

It is observed that at its stop frequency, the QH800 is characterized by a not negligible cx-polar level and an asymmetric co-polarized pattern (especially the E-Plane). It should be also noted that the spectrum is characterized by the presence of many odd and even |μ|-modes. As pointed out in [12], the even modes are those that generate the asymmetry on the radiation pattern and thus make the probe compensation more challenging.

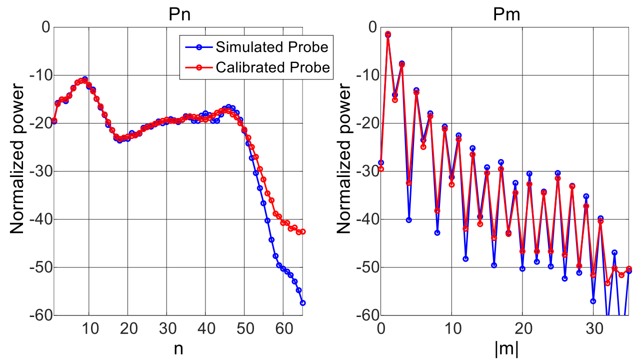

Fig. 4. Measured vs. calibrated spherical wave spectrum of the MVG QH800 higher order probe: Pn-modes (left), Pm-modes (right).

B. NF/FF Transformation Comparison

The NF/FF transformation results obtained from the processing of the measured NF data are reported in this section.

Fig. 5 shows the measured AUT directivity pattern comparison between reference (blue trace), NF/FF transformation without PC (black), NF/FF transformation with first order PC using simulated (red trace) and calibrated probe data (green trace). Focusing on the co-polarized pattern, the application of both first order PCs does not improve the Side Lobe Level (SLL) errors. The on-axis cx-polar discrimination (XPD) is instead improved by the application of the first order PC, especially if applied using the calibrated probe data. On the other hand, a not negligible residual error is present in the remaining part of the cx-polar pattern.

A similar comparison to the one shown in Fig. 5 is reported in Fig. 6, where probe corrected results are now obtained applying the full PC algorithm.

The agreement with the full probe corrected co-polarized patterns and the reference is excellent. The measurement accuracy on the SLL is almost equivalent considering the probe compensation performed with calibrated or simulated probe data.

Focusing on the cx-polar pattern, it can be observed that the full PC applied using the simulated probe data is capable to significantly improve the results. The on-axis XPD has in fact been improved of approximately 15 dB and the overall cx-polar performances have been lowered wrt the uncompensated results. Additional improvements on the cx-polar performances are obtained applying the full PC algorithm using the calibrated probe data. In this case, the on-axis XPD has further improved of approximately 7 dB wrt to the full PC applied using the simulated probe data. Moreover, as in the reference, an overall cx-polar pattern below 50 dB wrt peak almost everywhere has been obtained.

It should be noted that the slightly worse cx-polar performances obtained considering the simulated probe data in the compensation, are due to minor uncertainties in the probe manufacturing that are not accounted for in the full-wave simulation.

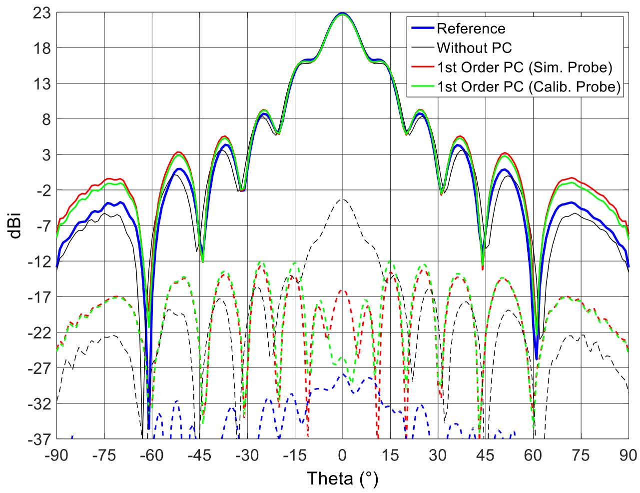

Fig. 5. Directivity H-Plane pattern comparison of the SGH820 @ 12 GHz measured with the QH800. Compensated results obtained with 1st order PC.

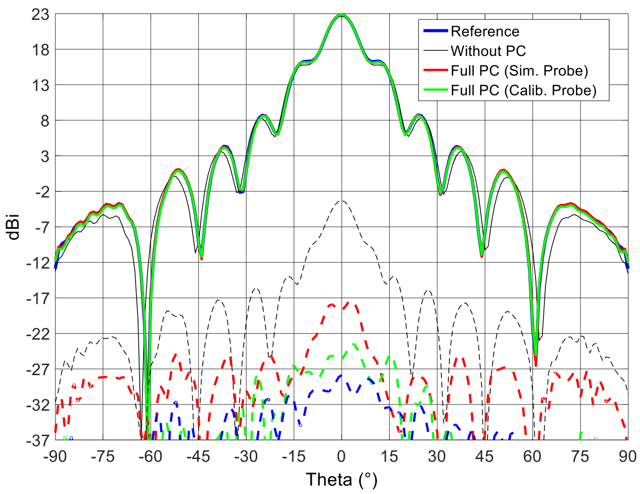

Fig. 6. Directivity H-Plane pattern comparison of the SGH820 @ 12 GHz measured with the QH800. Compensated results obtained with Full PC.

C. *Accuracy of the Results*

In order to quantify the accuracy of the achieved results some error metrics have been calculated and reported in Table 1.

TABLE I. ACCURACY OF THE RESULTS

	Dir. Error (dB)[a]	SLL EEL (dB)[b]	XPD (dB)[c]	Global EEL (dB)[d]
No PC	-0.19	-39.0	25.9	-26.0
1st order PC (Sim. Probe)	-0.16	-33.7	38.6	-39.0
1st order PC (Cal. Probe)	-0.14	-34.6	48.1	-39.7
Full PC (Sim. Probe)	+0.05	-54.3	41.6	-48.1
Full PC (Cal. Probe)	+0.03	-48.5	48.5	-50.3

a. Reference Directivity = 22.8 dBi;

b. SLL at θ = 37°, reference SLL = 18.5 dB;

c. Reference On-Axis XPD = 50.7 dB;

d. Computed considering amplitude and phase data.

The deviation of the peak directivities are reported in the second column. A higher error is obtained if the full PC is not considered but almost the same results are obtained applying it using calibrated or simulated probe data.

In the third column, the error on the SLL has been estimated computing the Equivalent Error Level (EEL) [18] with the following formula:

$$e_i(\theta,\phi) = \left| \frac{E(\theta,\phi) - \tilde{E}(\theta,\phi)}{E(\theta,\phi)} \right| \cdot \frac{\left|\tilde{E}(\theta,\phi)\right|}{\left|\tilde{E}(\theta,\phi)\right|_{MAX}} \qquad (2)$$

where:

- $\tilde{E}(\theta,\phi)$ is the reconstructed pattern,
- $E(\theta,\phi)$ is the reference pattern

As can been seen, the application of the full PC allows to obtain very accurate SLL results both considering the calibrated and simulated probe characterization. Instead, as evident from Fig. 5, the first order PC applied to this test case is not able to return enough accurate SLL results.

The on-axis cx-polar discrimination (XPD) is reported in the fourth column. As already pointed out, the improvements obtained using calibrated probe data rather that simulated data are remarkable since almost the same reference on-axis XPD is reached.

The global EEL, obtained averaging the output of (2) among any (θ,φ) coordinate of the patterns, is reported in the fifth column. Such a metric has been computed accounting for both the amplitude and the phase data of the patterns. As expected, the best accuracies are obtained applying the full PC using calibrated and simulated probe data. The global EEL is slightly better if calibrated probe data are used in the compensation.

IV. Conclusion

In this paper a comparative investigation of full and first order probe correction using calibrated or simulated probe data has been carried out. The experimental validation has been conducted measuring a standard gain antenna (SGH820) as AUT with a higher order probe (QH800). The investigation has been performed considering both first order and full PC algorithms.

The considered full PC approach is based on the modification of the SWE basis functions, which are properly elaborated taking into account the effect of the probe, and then used in the field expansion, directly compensating for the probe pattern without any restriction of the probe itself.

The comparison between probe compensations performed with calibrated and simulated probe characteristics has shown very accurate co-polar results in both cases involving the full PC algorithm. A non-negligible residual error is instead shown if first order PC is applied either with calibrated or simulated probe data.

Excellent cx-polar results are obtained applying the full PC with simulated probe representation. Considering the calibrated probe, the cx-polar performance is further improved almost reaching the reference. The slightly worse cx-polar performances obtained considering the simulated probe representation in the compensation are due to minor uncertainties in the probe manufacturing that are not accounted for in the full-wave simulation.

References

[1] ANSI/IEEE Std 149-1979 “IEEE Standard Test Procedures for Antennas”

[2] IEEE Std P1720™/D2 (Draft) “Recommended Practice for Near-Field Antenna Measurements”

[3] J. E. Hansen (ed.), Spherical Near-Field Antenna Measurements, Peter Peregrinus Ltd., on behalf of IEE, London, United Kingdom, 1988

[4] L. J. Foged, A. Giacomini, S. Pivnenko, “Wide band dual polarized probes for near and farfield measurement systems”, AMTA 2007, November 4-9, 2007 St. Louis, MO, USA.

[5] L. J. Foged, A. Giacomini, R. Morbidini, “Probe Performnce Limitation Due to Excitation Errors in External Beam Forming Network”, AMTA 2011, Colorado, USA

[6] T. A. Laitinen, S. Pivnenko, and O. Breinbjerg, “Iterative probe correction technique for spherical near-field antenna measurements,” IEEE Antennas Wireless Propag. Lett., vol. 4, 2005.

[7] T. A. Laitinen and O. Breinbjerg, “A first/third-order probe correction technique for spherical near-field antenna measurements using three probe orientations,” IEEE Trans. Antennas Propag., vol. 56, pp. 1259–1268, May 2008.

[8] T. A. Laitinen, “Double φ-step θ-scanning technique for spherical near-field antenna measurements”, IEEE Transactions on Antennas and Propagation, Vol. 56, pp. June 2008.

[9] Tommi Laitinen, Sergey Pivnenko, Jeppe Majlund, Olav Breinbjerg “Theory and Practice of the FFT/Matrix Inversion Technique for Probe-Corrected Spherical Near-Field Antenna Measurements With High-Order Probes”, IEEE Transactions on Antennas and Propagation, Vol. 58, No.8, August 2010.

[10] C. H. Schmidt, M. M. Leibfritz, and T. F. Eibert, “Fully probe-corrected near-field to far-field transformation employing plane waveexpansion and diagonal translation operators,” IEEE Trans. Antennas Propag., vol. 56, pp. 737–746, Mar. 2008.

[11] L. J. Foged, F. Saccardi , A. Giacomini, “Higher Order Versus First Order Probe Correction Techniques Applied to Experimental Spherical NF Antenna Measurements”, EuCAP 2016, Davos, Switzerland.

[12] L. J. Foged, F. Saccardi , A. Giacomini, “Probe Correction Technique of Arbitrary Order for High Accuracy Spherical Near Field Antenna Measurements”, AMTA 2016, Austin, Texas, USA.

[13] http://www.mvg-world.com/en/system/files/datasheet_antenna_2016_hd_open_boundary_quadridge_horns.pdf

[14] http://www.kuka-robotics.com/res/sps/6b77eeca-cfe5-42d3-b736-af377562ecaa_PF0055_KR_5_sixx_en.pdf

[15] G. Giordanengo, F. Vipiana, L.J. Foged, L. Scialacqua, F. Saccardi, M. Bandinelli, M. Bercigli, G. Guida, M. Sabbadini, G. Vecchi, “Hybrid Measurement/Simulation Approach for Satellite AIT/AIV”, 35th ESA Antenna Workshop, ESA/ESTEC, Noordwijk, The Netherlands

[16] http://www.mvg-world.com/en/system/files/datasheet_antenna_2016_hd_dual_polarizd_open_ended_waveguide_with_interchangeable_apertures.pdf

[17] https://www.cst.com/

[18] M.A. Saporetti, L.J. Foged, M. Sierra Castañer, E. Jørgensen, T. Voigt, A. Michel, D. Tallini, B. Kolundzija, M. Böttcher, A. Wien, M.Orefice, G. Giordanengo, G. Dassano, J. M. Serna, F. Catedra, A. Somolinos, J. Moreno, I. Gonzales, "Measurements and Simulations Correlation of High Reliability Reflector Antenna", EuCAP2016, Davos, April 2016